Table S1. Scoring criteria of the bladder phenotype

Phenotype	Definition	Criteria
Bladder phenotype	Overall state of the urothelial tumorigenesis	Minimal changes, urothelial hyperplasia or atypia, dysplastic urothelium or carcinoma in situ (CIS), tumour
Invasiveness	State of the basement membrane and invasion of tumour cells	Normal basement membrane, ambiguous basement membrane, breakage of basement membrane, stromal invasion, muscle invasion.
Squamous transformation	Squamous appearance of cells and keratinization in the urothelium or in the tumour	None, mild or present locally in a small area, advanced, fully transformed and often keratinized.

Table S2. Antibodies used for IHC and conditions for staining

Antibody	Supplier	Catalogue number	Type	Pre-treatment	AR buffer	Antibody dilution
Caspase 3	Cell Signaling	9661	Rabbit monoclonal		pH 6	1:200
CD3	Vector Laboratories	VP-RM01	Rabbit monoclonal		pH 8	1:100
CD4	eBioscience	14-9766	Rat monoclonal		pH 8	1:200
CD8α	eBioscience	14-0808	Rat monoclonal		pH 8	1:200
Cxcr2	R&D Systems	MAB2164	Rat monoclonal		pH 6	1:200 (overnight)
F4/80	Abcam	ab6640	Rat monoclonal		pH 6	1:400
FoxP3	Abcam	ab54501	Rabbit polyclonal		pH 8	1:500
FoxP3	eBioscience	14-5773-82	Rat monoclonal		pH 8	1:200
Granzyme B	AbCam	ab4059	Rabbit polyclonal		pH 8	1:800
Ki67	Novacastra	NCL-Ki67p	Rabbit polyclonal		pH 6	1:1000
Ly6G (1A8)	BioXcell	BE0075-1	Rat monoclonal		pH 8	1:6000
MPO (α-)	DAKO	A0398	Rabbit polyclonal		pH 8	1:1000
NIMP	AbCam	ab2557	Rat monoclonal	10 mg/ml Proteinase K for 10 min at 37°C	N/A	1:50
S100A9	Abcam	ab105472	Rat monoclonal		pH 6	1:100

*Supplier details are AbCam (Cambridge, UK), BioXcell (West Lebanon, New Hampshire, USA), Cell Signaling Technology (London, UK), DAKO (Agilent, Stockport, UK), eBioscience (VWR, Lutterworth, UK), Novacastra (Newcastle upon Tyne, UK), R&D Systems (Minneapolis, Minnesota, USA), Vector Laboratories (Peterborough, UK).

Table S3. mRNA expressions in *Cxcr2 flox* tumours comparing to *wildtype* tumours (log2 fold)
The mRNA expressions in tumours were investigated in *Cxcr2 flox* comparing to *wildtype* mice at 20 weeks, using RT2 Profiler Mouse Cancer Inflammation & Immunity Crosstalk PCR Array (Qiagen, Manchester, UK). Total RNA was extracted from tumours n=3 *wildtype*, n=2 *Cxcr2 flox* (males). The fold changes were shown as log2 values normalised by house keeping genes, *Actb, B2m, GusB, Gapdh, Hsp90 and Mgdc.* Within each category, the genes are sorted from high to low expression. Genes mentioned in the main text are highlighted.

Gene category	*House keeping genes for normalization*	*actb*	*b2m*	*gapdh*	*gusb*	*Hsp90*	*mgdc*
Immunostmulatory	*il2*	5.6997	4.1917	4.18153	3.7012	2.85353	2.3072
	il12a	3.97462	2.46662	2.45645	1.97612	1.12845	0.58212
	il15	3.82649	2.31849	2.30832	1.82799	0.98032	0.43399
	ccl2	3.16197	1.65397	1.64381	1.16347	0.31581	-0.2305
	il12b	3.03703	1.52903	1.51886	1.03853	0.19086	-0.3555
	ifng	2.52401	1.51051	0.49851	2.02951	-0.4955	1.03251
	tnf	1.66768	0.15968	0.14952	-0.3308	-1.1785	-1.7248
Immunosuppressive	*il5*	5.86582	4.35782	4.34766	3.86732	3.01966	2.47332
	il4	5.84878	4.34078	4.33061	3.85028	3.00261	2.45628
	pdcd1/Pd-1	4.55245	3.04445	3.03428	2.55395	1.70628	1.15995
	mif	4.18447	2.67647	2.66631	2.18597	1.33831	0.79197
	csf2	3.99555	2.48755	2.47738	1.99705	1.14938	0.60305
	il13	3.56713	2.05913	2.04896	1.56863	0.72096	0.17463
	ido1	3.49916	1.99116	1.98099	1.50066	0.65299	0.10666
	ptgs2 (Cox2)	3.19151	1.68351	1.67334	1.19301	0.34534	-0.201
	cd274/Pd-L1	2.84178	1.33378	1.32361	0.84328	-0.0044	-0.5507
	nos2	2.83716	1.32916	1.31899	0.83866	-0.009	-0.5553
	il10	2.64438	1.13638	1.12621	0.64588	-0.2018	-0.7481
	vegfa	2.19704	0.68904	0.67887	0.19854	-0.6491	-1.1955
	cxcl5	2.15769	0.64969	0.63952	0.15919	-0.6885	-1.2348
	cxcl12	2.00603	0.49803	0.48786	0.00753	-0.8401	-1.3865
	tgfb1	1.50918	0.00118	-0.009	-0.4893	-1.337	-1.8833
	ctla4	1.49325	-0.0148	-0.0249	-0.5053	-1.3529	-1.8993
Chemokines (not listed above)	*cxcl11*	4.37147	2.86347	2.8533	2.37297	1.5253	0.97897
	ccl28	4.01374	2.50574	2.49557	2.01524	1.16757	0.62124
	ccl22	3.88579	2.37779	2.36762	1.88729	1.03962	0.49329
	ccl5	3.84565	2.33765	2.32748	1.84715	0.99948	0.45315
	ccl4	3.83153	2.32353	2.31336	1.83303	0.98536	0.43903
	ccl20	2.84312	1.33512	1.32495	0.84462	-0.0031	-0.5494
	cxcl2	2.64856	1.14056	1.13039	0.65006	-0.1976	-0.7439
	cxcl10	2.17842	0.67042	0.66025	0.17992	-0.6677	-1.2141
	cxcl9	1.49309	0.47959	-0.5324	0.99859	-1.5264	0.00159
	cxcl1	1.29028	-0.2177	-0.2279	-0.7082	-1.5559	-2.1022
Chemokine & Interleukin Receptors	*ccr2*	6.68442	5.17642	5.16626	4.68592	3.83826	3.29192
	ccr10	5.35177	3.84377	3.83361	3.35327	2.50561	1.95927
	Ackr3 (cxcr7)	4.98844	3.48044	3.47027	2.98994	2.14227	1.59594
	cxcr4	3.99653	2.48853	2.47837	1.99803	1.15037	0.60403
	ccr7	3.84401	2.33601	2.32585	1.84551	0.99785	0.45151
	ccr4	3.83221	2.32421	2.31404	1.83371	0.98604	0.43971
	ccr9	3.5467	2.0387	2.02854	1.5482	0.70054	0.1542
	cxcr5	3.34192	1.83392	1.82375	1.34342	0.49575	-0.0506
	cxcr1	3.2162	1.7082	1.69804	1.2177	0.37004	-0.1763
	cxcr3	2.69462	1.18662	1.17645	0.69612	-0.1515	-0.6979
	ccr5	2.55245	1.04445	1.03429	0.55395	-0.2937	-0.84
	ccr1	2.33495	0.82695	0.81678	0.33645	-0.5112	-1.0575
	cxcr2	2.17258	0.66458	0.65441	0.17408	-0.6736	-1.2199
	il1r1	1.5042	-0.0038	-0.014	-0.4943	-1.342	-1.8883

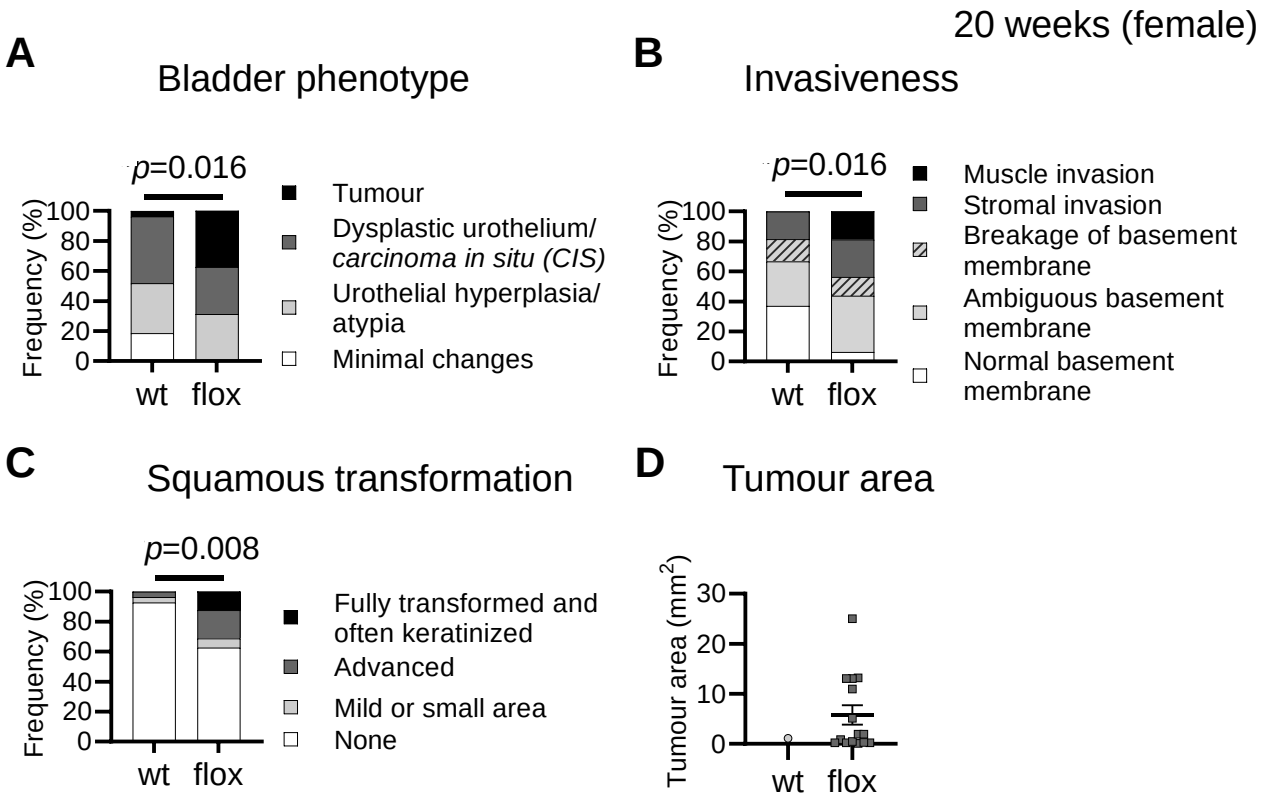

Figure S1. Phenotype of the bladder tumours in female mice at 20 weeks from the start of carcinogen treatment. The overall bladder phenotype (**A**), invasiveness (**B**) and squamous transformation of the urothelium and tumours (**C**) of female mice at 20 weeks are expressed as frequency of observation (%) comparing *wild-type* and *Cxcr2 flox* mice (*wt*, n=27; *flox*, n=16). (**D**) The tumour area in a representative section (*wt*, n=1; *flox*, n=16). The bars represent the means with standard deviation in D. The *p*-values were determined using the Mann-Whitney test and indicated where significant ($p<0.05$).

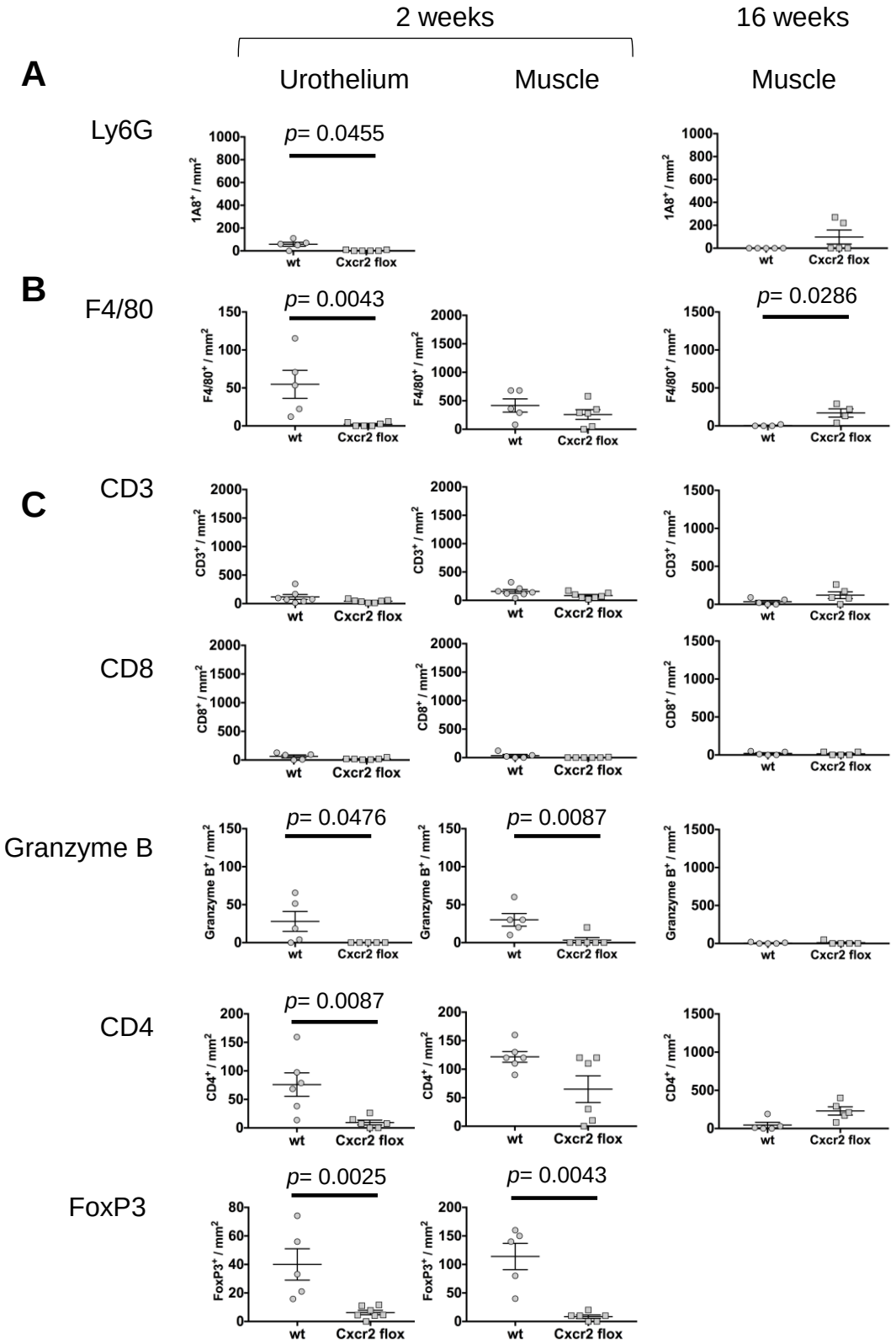

Figure S2. Infiltration of Ly6G$^+$ neutrophils, macrophages and T cells in *LysMCre Cxcr2$^{flox/flox}$* bladder urothelium and muscle layer at 2 and 16 weeks. Ly6G$^+$ neutrophils (**A**), macrophages (F4/80$^+$) (**B**), and T cell populations (**C**), quantified in the *wildtype* (wt) and *LysMCre Cxcr2$^{flox/flox}$* (Cxcr2 flox) bladders at 2 and 16 weeks from the start of OH-BBN treatment. A data point is from each mouse (*wt* n=5, *flox* n=6 at 2 weeks; *wt* n=5, *flox* n=5 at 16 weeks). The bars represent the means with standard deviation. The *p*-values (Mann-Whitney test) are indicated where significant ($p < 0.05$).

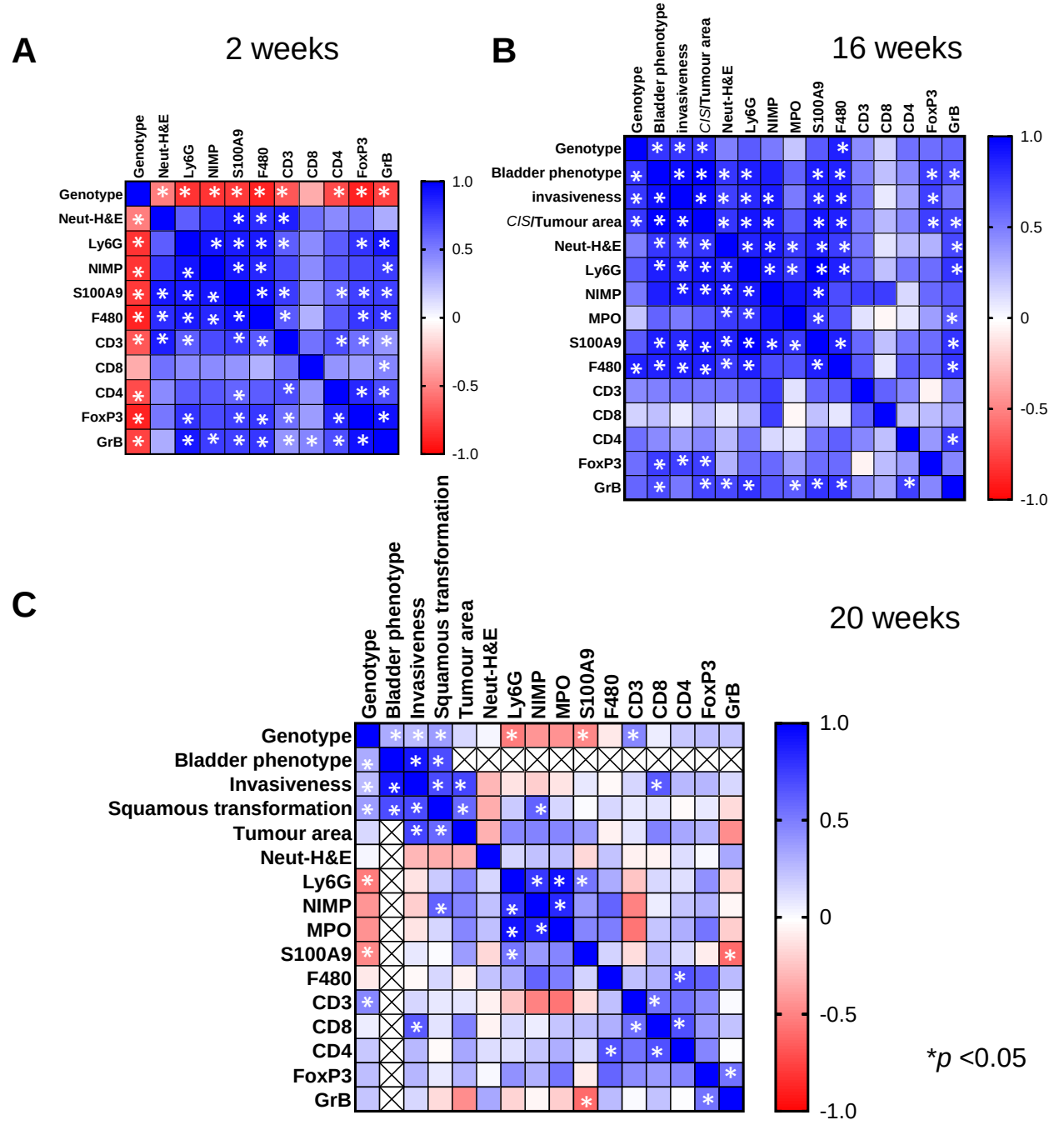

Figure S3. Spearman correlation analysis comparing genotype, bladder phenotype, and infiltration of neutrophils, macrophages and T cells. The increase in TILs observed at 20 weeks (Figure 2C) could be caused by *Cxcr2* deletion or by the enhanced tumour pathogenesis in *Cxcr2 flox* mice. The correlation among genotype, tumour phenotype and immune cell levels was analysed in male stroma at 2 weeks (**A**), 16 weeks (**B**), and 20 weeks (**C**), and presented as heatmaps of Spearman correlation coefficient (r) values. The values are marked as an asterisk (*) when $p<0.05$. The values ranged as $0 < r < 1$ (blue) indicate that the two variables tend to increase or decrease similarly, while the values ranges as $-1 < r < 0$ (red) indicate that the two variables tend to have an inverse correlation. In panel C, coefficients were not evaluated in X, as the analysis was performed in the single category "tumour" within the bladder phenotype. (A) At 2 weeks, the levels of neutrophils, macrophages and T cells correlated with *Cxcr2* deletion in a statistically significant manner. (B) At 16 weeks, bladder phenotype and levels of macrophages correlated with *Cxcr2* deletion, however, levels of neutrophils and T cells were no longer associated with *Cxcr2* deletion, but correlated with bladder phenotype. (C) At 20 weeks, bladder phenotype, particularly invasiveness and squamous transformation, $Ly6G^+$, $S100A9^+$ neutrophils, and $CD3^+$ T cells correlated with *Cxcr2* deletion. Little correlation was found between TILs and invasiveness or squamous transformation. Therefore, rather than the state of tumour progression, *Cxcr2* deletion may have had more influence on the changes in $CD3^+$ T cells.

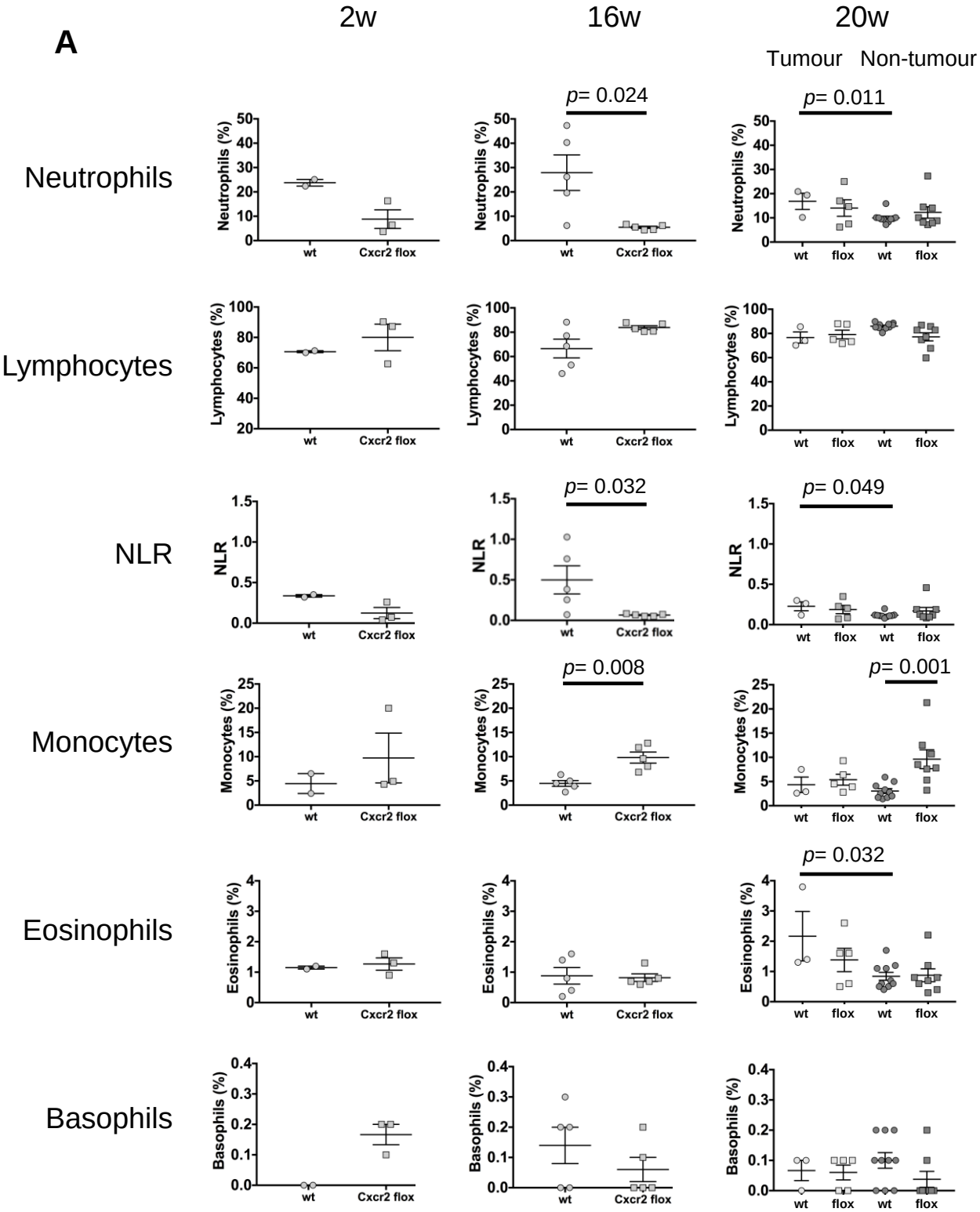
A
2w
16w
20w
Tumour
Non-tumour
Neutrophils
Lymphocytes
NLR
Monocytes
Eosinophils
Basophils
p= 0.024
p= 0.011
p= 0.032
p= 0.049
p= 0.008
p= 0.001
p= 0.032
wt
Cxcr2 flox
flox

(Figure S4)

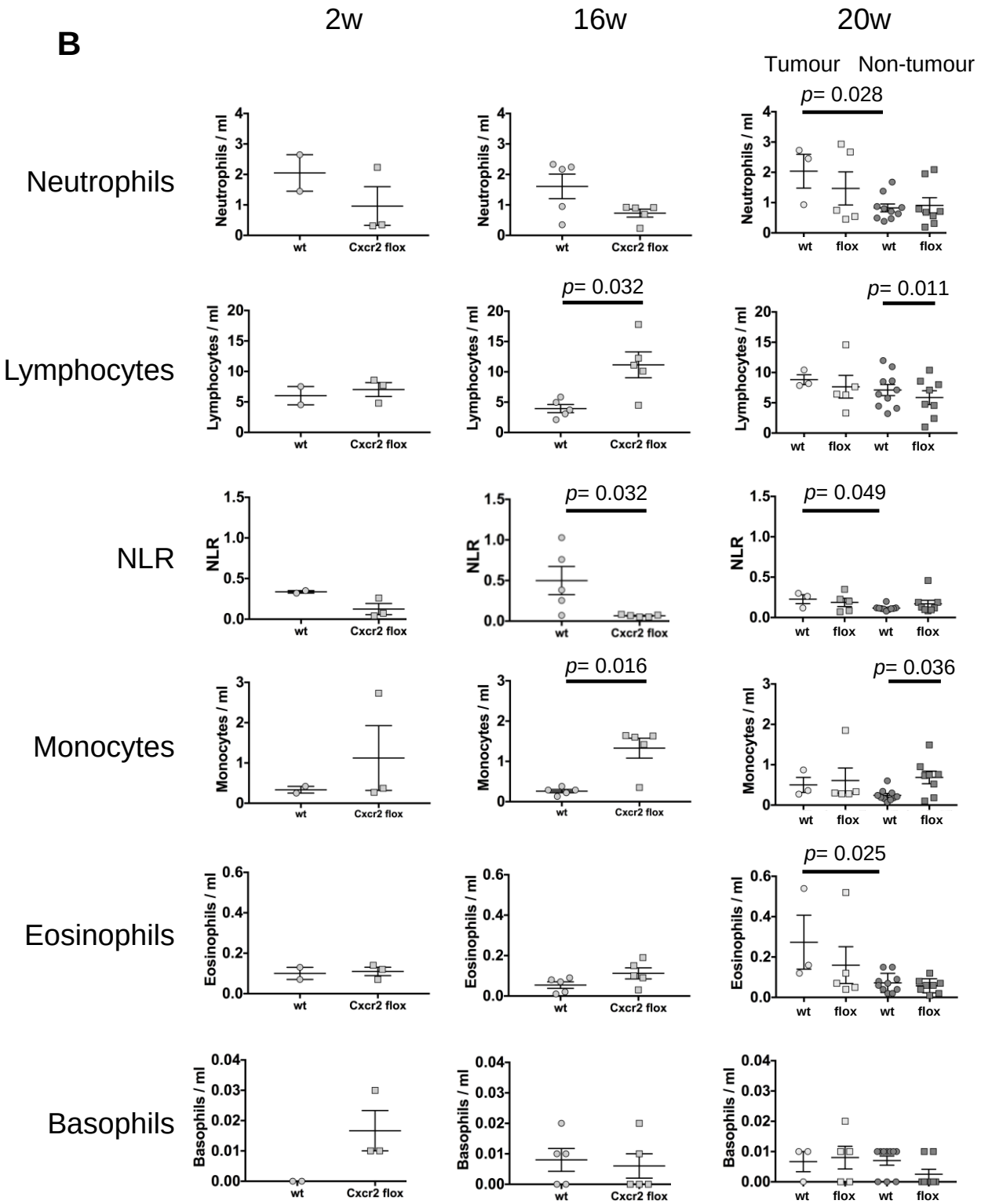

Figure S4. **The effects of *Cxcr2* deletion on the levels of immune cells in circulation.** The levels of neutrophils, lymphocytes, neutrophil-to-lymphocyte ratio (NLR), monocytes, eosinophils and basophils in *wild-type* and *Cxcr2 flox* mice are presented as a population within whole blood cell counts (%) (**A**) and as a density (cells/ml) (**B**). Mice with tumours and those without (non-tumour) were analysed at 20 weeks. A data point is from each mouse (*wt* n=2, *flox* n=3 at 2 weeks; *wt* n=5, *flox* n=5 at 16 weeks; *wt* with tumour n=3, *flox* with tumour n=5, *wt* non-tumour n=10, *flox* non-tumour n=8). The NLR values are the same in A and B. The bars represent the means with standard deviation. The *p*-values (Mann-Whitney test for non-parametric distribution) are indicated where significant ($p < 0.05$).

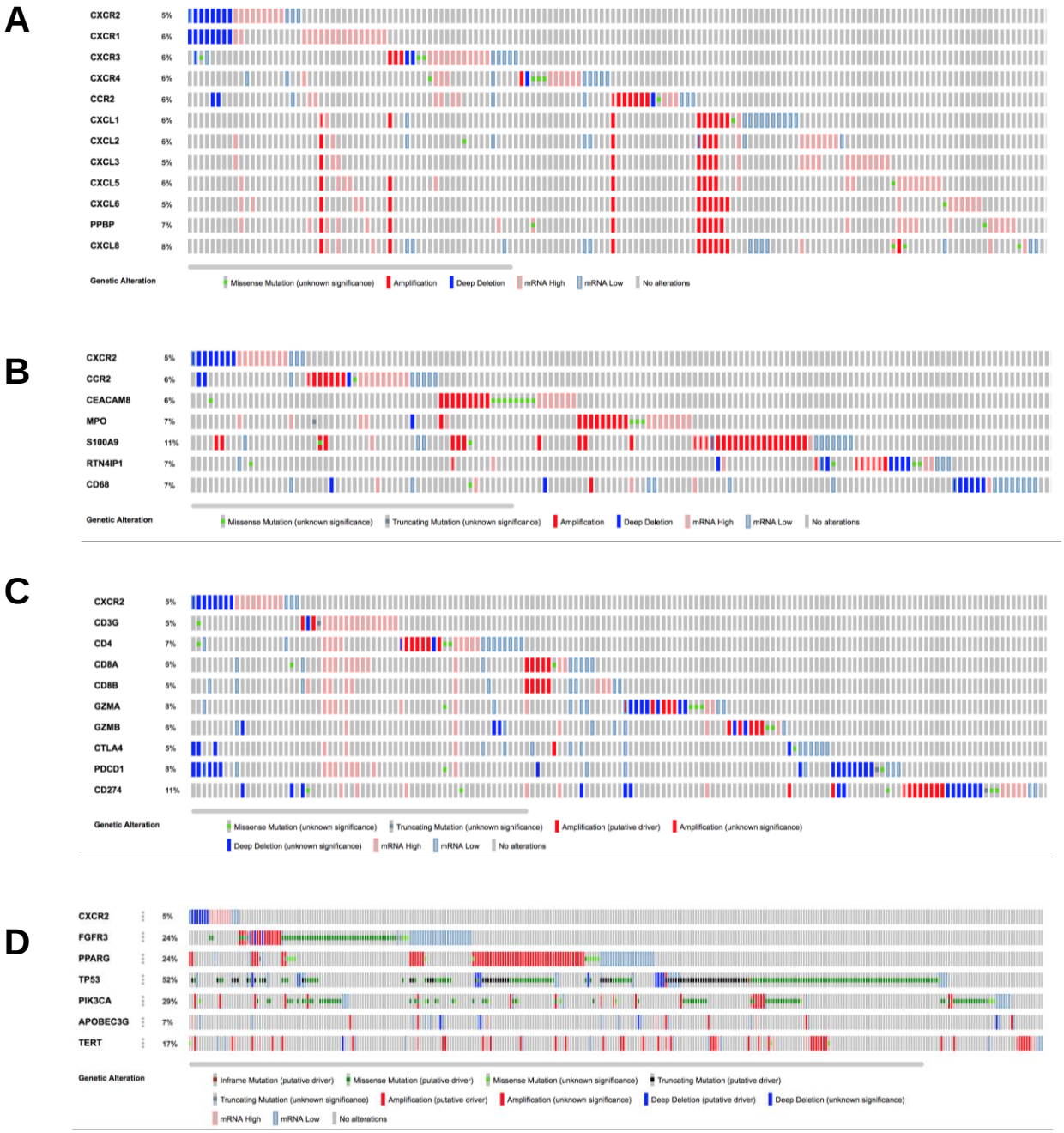

Figure S5. OncoPrints of *CXCR2* genomic alterations and mRNA levels in a TCGA human MIBC cohort. (**A**) Using the cBioPortal, OncoPrinter, *CXCR2* genomic and mRNA expression levels were compared against *CXCR* family members, chemokine receptor, *CCR2*, and CXC ligands in the case set "complete samples n=404". Alterations were found in 149/404 (37%) of the samples. Deep deletions of *CXCR2* occurred together with that of *CXCR1* in n=8 cases, and with *CCR2* (n=2). (**B**) *CXCR2* was compared against *CCR2* and genes expressed in neutrophils and macrophages. Alterations were found in 149/404 (37%). Deep deletion of *CXCR2* occurred together with amplification of *S100A9* (n=2). (**C**) *CXCR2* was compared with genes expressed in T-cells. Alterations were found in 155/404 (38%). Deep deletions occurred together in *CXCR2, CTLA4* (n=3) and *PDCD1* (PD-1) (n=6) (**D**) *CXCR2* was compared against oncogenes and tumour suppressor known in bladder cancer. Genes were altered in 341/404 (84%). Deep deletion of *CXCR2* occurred together with amplification of *PPARG* (n=2), putative driver mutations of *TP53* (n=2), and amplification of *PIK3CA* and *TERT* (n=1). Deep deletion of *CXCR2* was mutually exclusive with *FGFR3* genomic alterations.

A

TCGA muscle invasive bladder cancer (Cell, 2017) (n=412)

	Sex	Age	Disease Stage	Tumor Stage	Metastasis Stage	Lymph Node Stage	Histologic Grade	Mutation Count
Spearman r	0.022	-0.105	-0.110	-0.002	-0.236	-0.073	-0.216	-0.149
p	0.655	0.036	0.029	0.972	0.001	0.168	1.484E-05	0.003

B

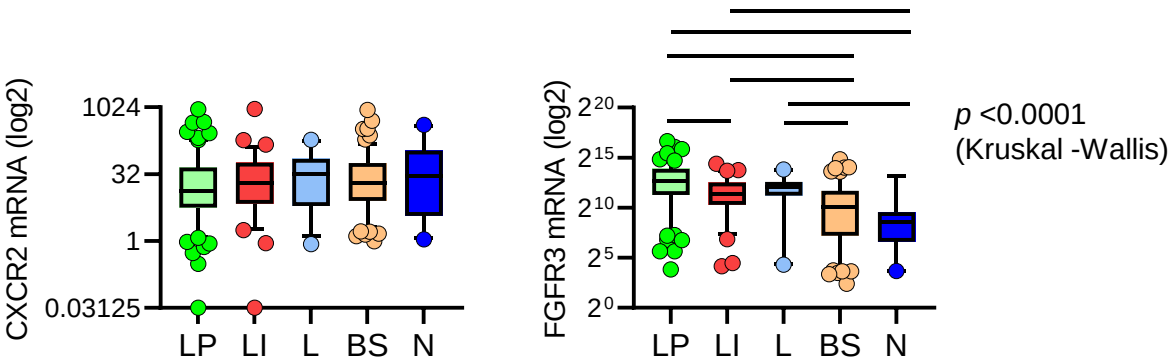

Figure S6. Clinicopathological characteristics and the MIBC molecular subtypes associated with *CXCR2* expression. (**A**) Correlation of *CXCR2* mRNA expression levels to clinicopathological characteristics was analysed in the Bladder Cancer, TCGA Cell 2017 cohort (n=412). The Spearman correlation coefficient r in the range of 0 < r <1 indicates that the two variables tend to increase or decrease similarly, while the values ranges as -1 < r <0 indicate that the two variables tend to have an inverse correlation. The *p* values of <0.05 are highlighted in red. (**B**) Expression levels of *CXCR2* and *FGFR3* in the TCGA MIBC molecular subtypes (mRNA Cluster). Box plots are with a line at median and whiskers at 5-95 percentile. Analysis was performed on cases with molecular subtype information and mRNA data were available (n=400). Overall significance was observed when comparing *FGFR3* expression levels, but not *CXCR2* (Kruskal-Wallis test). Dunn's multiple comparison test was used for comparisons between each subtype. For *FGFR3*, bars are shown when the *p* value was <0.01. LP, luminal-papillary; LI, luminal-infiltrated; L, luminal; BS, basal/squamous; N, neuronal.

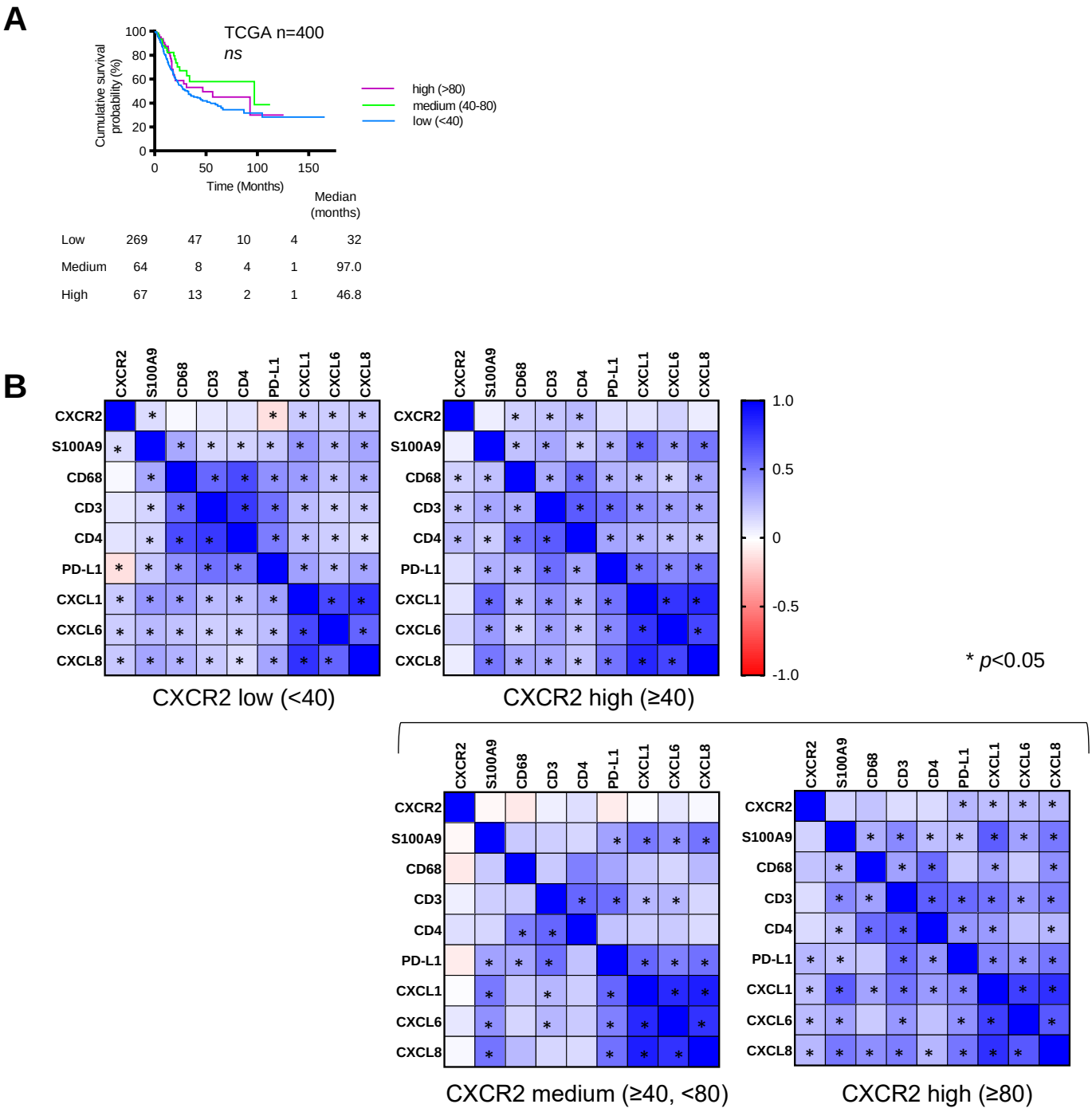

Figure S7. Survival analysis of the TCGA MIBC dataset and correlation of mRNA expression levels of *CXCR2, S100A9*, *CD68,* T cells, *PD-L1,* and CXC ligands. (**A**) Survival analysis was performed in the Bladder Cancer, TCGA, Cell 2017 cohort, with *CXCR2* mRNA expression and overall survival data was available (n=400), categorised according to low (<40, n=269), medium (≥40, <80, n=64), and high (≥80, n=67) *CXCR2* mRNA expression. The difference in the survival among the categories was not statistically significant (*ns*). (**B**) Spearman correlation analysis was first analysed in *CXCR2* expression categories "low" (<40, n=269) and "high" (≥40, n=129) (upper panels). The "high" category was further divided as "medium" (≥40, <80, n=64) and "high" (≥80, n=65) (lower panels). The heatmap indicates Spearman r co-efficient, where -1 < r < 0 (red) represents inverse correlation, while 0 < r < 1 (blue), positive correlation. Asterisks (*) indicate where correlation was statistically significant with a *p*-value < 0.05.

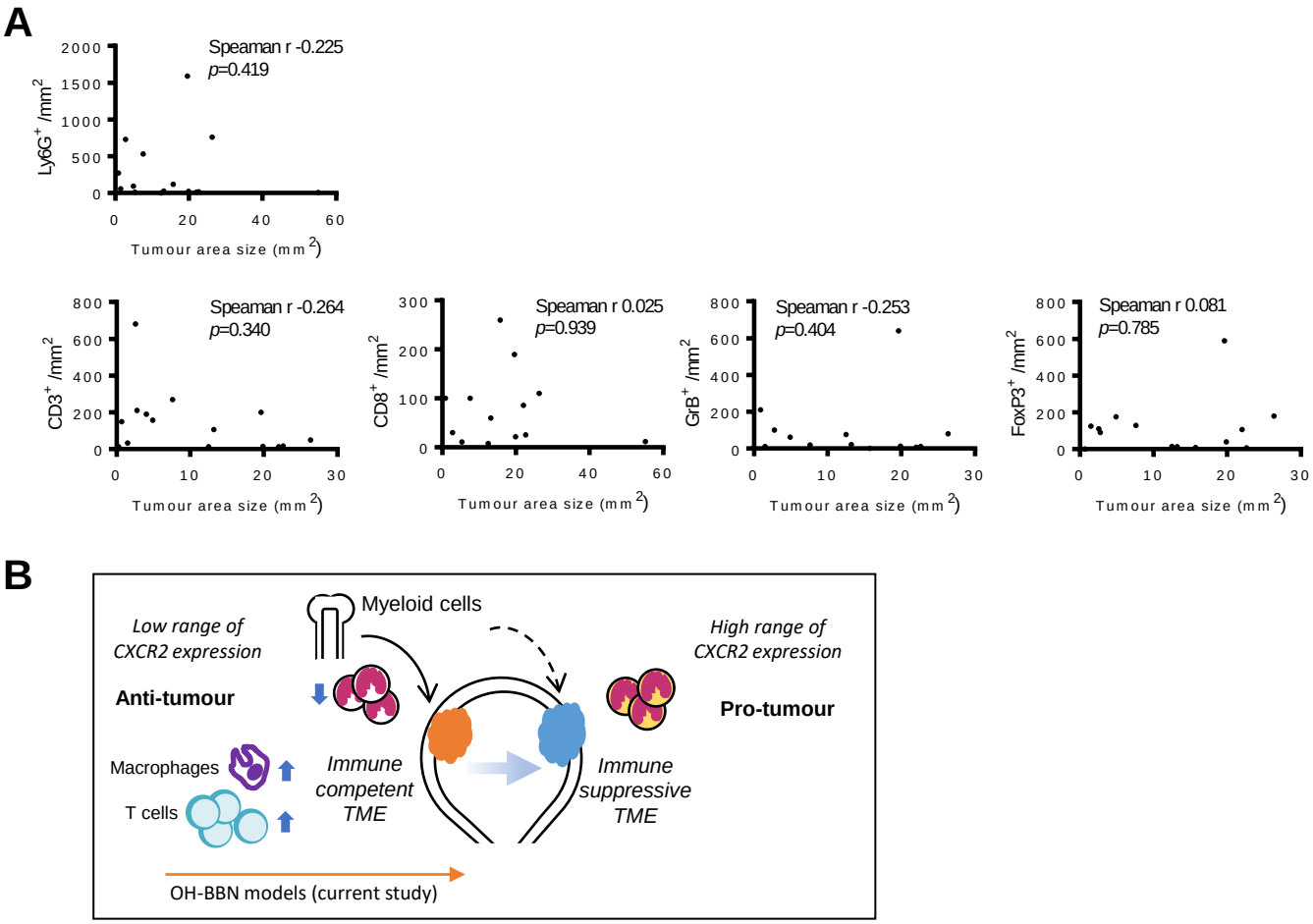

Figure S8. Status of immune suppression in tumours developed in OH-BBN treated mice. (**A**) Relationship between tumour area size and immune cell density was evaluated in *Wild-type* mice that developed tumour at 20 weeks (n=12) and beyond 20 weeks (n=10) from the start of OH-BBN treatment. *Wild-type* mice were treated with 0.05% OH-BBN for 10 weeks. Mice aged beyond 20 weeks (21 – 43 weeks) were monitored by ultrasound imaging for the presence of bladder tumours and culled when mice showed clinical signs of bladder tumour, such as haematuria and weight loss. Tumour area was quantified by QuPath on a representative H&E-stained section. Immunohistochemistry was performed for Ly6G, CD3, CD8, Granzyme B (GrB), and FoxP3. Cell density was determined in the tumour using QuPath. Correlation was expressed as Spearman r co-efficient and the *p* values (highlighted in red when p<0.05). **(B)** Overview of the role of CXCR2 in bladder cancer and immune suppressive status in the mouse model. Our model of *Cxcr2* deletion reflects human bladder cancer with low range of *CXCR2* expression (left). *Cxcr2* deletion suppressed acute inflammation during tumour initiation, leading to an increased tumour burden. Our OH-BBN induced model does not fully develop immunosuppressive microenvironment in the tumour. In tumours with a higher level of *CXCR2* expression in humans (right), CXCR2 may play a pro-tumour role, as previously reported (29-31).